



## ORIGINAL ARTICLE

# Adsorption behavior and corrosion inhibitive potential of xanthene on mild steel/sulphuric acid interface

N.O. Obi-Egbedi <sup>a</sup>, I.B. Obot <sup>b,\*</sup>

<sup>a</sup> Department of Chemistry, University of Ibadan, Ibadan, Nigeria

<sup>b</sup> Department of Chemistry, Faculty of Science, University of Uyo, P.M.B 1017, Uyo, Akwa Ibom State, Nigeria

Received 1 July 2010; accepted 8 August 2010

Available online 11 August 2010

## KEYWORDS

Xanthene;  
Mild steel corrosion inhibitors;  
Density functional theory (DFT);  
Sulphuric acid

**Abstract** The inhibition of xanthene (XEN) on the corrosion of mild steel in 0.5 M H<sub>2</sub>SO<sub>4</sub> was studied by gravimetric and UV–visible spectrophotometric methods at 303–333 K. Results obtained show that XEN act as inhibitor for mild steel in H<sub>2</sub>SO<sub>4</sub> solution. The inhibition efficiency was found to increase with increase in XEN concentration but decreased with temperature. Activation parameters and Gibbs free energy for the adsorption process using Statistical Physics were calculated and discussed. The corrosion process in 0.5 M H<sub>2</sub>SO<sub>4</sub> in the absence and presence of XEN follows zero-order kinetics. The UV–visible absorption spectra of the solution containing the inhibitor after the immersion of mild steel specimen indicate the formation of a XEN–Fe complex. Quantum chemical calculations using DFT were used to calculate some electronic properties of the molecule in order to ascertain any correlation between the inhibitive effect and molecular structure of xanthene.

© 2010 King Saud University. Production and hosting by Elsevier B.V. All rights reserved.

## 1. Introduction

Corrosion of steel is the most common form of corrosion, especially in acid solution. It has practical importance, for example, in the acid pickling of iron and steel, chemical clean-

ing of scales in metallurgy, in the oil recovery and petrochemical industry (Ashassi-Sorkhabi et al., 2009). The corrosion of iron materials is interpreted in terms of electrochemical reactions of local cells operating on the corroding surface. The overall corrosion reaction may be split into the anodic and cathodic partial reactions (Solomon et al., 2010):



Thus, the attack of metal is mainly linked to the reduction of hydrogen ions in acid solution (Benabdellah and Hammouti, 2005). The isolation of a metal from this corrosive agent is the most effective way to prevent electrochemical corrosion. Among the different methods available (Jones, 1992; Fontana, 1986), the use of corrosion inhibitors is usually the most appropriate way to achieve this objective.

\* Corresponding author. Tel.: +234 8067476065.  
E-mail address: proffoime@yahoo.com (I.B. Obot).



Detailed studies from our laboratory (Obot et al., 2009, 2010; Obot and Obi-Egbedi, 2008a,b, 2009, 2010a,b,c; Obot, 2009; Ebenso et al., 2008) reveal that most of the efficient inhibitors are organic compounds which mainly contain oxygen, sulphur, nitrogen atoms and multiple bonds in the molecule through which they are adsorbed on metal surface. The effectiveness of the adsorption depends on the nature and surface charge of the metal, the corroding medium and the chemical structure of the inhibitor molecule such as functional groups, aromaticity,  $\pi$ -orbital character of the donating electron, steric factor, and electron density at the donor atoms (El-Naggar, 2007; Umoren and Ebenso, 2007; Lebrini et al., 2006; Bentiss et al., 2000).

Xanthene (9-H-xanthene or 10H-9-oxaanthracene) is a yellow organic heterocyclic compound. Its chemical formula is  $C_{13}H_{10}O$ . Its melting point is 101–102 °C and its boiling point is 310–312 °C. Xanthene is used as a fungicide and is also a useful intermediate in organic synthesis. Among other uses are the basis of a class of dyes which includes fluorescein, eosins and rhodamines (Wikipedia encyclopedia, 2010). The choice of xanthene for the present investigation was based on the consideration that it contains several  $\pi$ -electrons and oxygen heteroatom, which can induce greater adsorption of the inhibitor molecule onto the surface of mild steel. Furthermore, the molecule is planar and has a higher molecular weight (182.22 g/mol) which can effectively cover the metal surface, thus, isolating the metal from the aggressive acidic medium.

The aim of this paper therefore is to explore the use of xanthene as corrosion inhibitor for mild steel surface in sulphuric acid solution using gravimetric method. The effect of temperature on corrosion and inhibition processes are thoroughly assessed and discussed. Kinetic and thermodynamic parameters were also calculated and discussed. UV-Vis spectroscopy together with quantum chemical study using density functional theory were further employed to provide additional insight into the mechanism of inhibitory action.

## 2. Experimental method

### 2.1. Material

Test was performed on a freshly prepared sheet of mild steel of the following composition (wt.%): 0.13% C, 0.18% Si, 0.39% Mn, 0.40% P, 0.04% S, 0.025% Cu, and bal Fe. The metal specimens were prepared, degreased and cleaned as previously described (Obot et al., 2010; Obot and Obi-Egbedi, 2010a).

### 2.2. Inhibitor

Xanthene (XEN) was purchased from Sigma-Aldrich and used as inhibitor. Stock solution was made in 10:1 water:methanol mixture to ensure solubility (Ahmad and Quraishi, 2010). This stock solution was used for all experimental purposes. Fig. 1 shows the molecular structure of XEN.

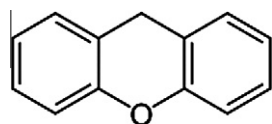


Figure 1 Molecular structure of xanthene (XEN).

### 2.3. Solutions

The aggressive solutions, 0.5 M  $H_2SO_4$  were prepared by dilution of analytical grade 98%  $H_2SO_4$  with distilled water. The concentration range of XEN prepared and used was  $2 \times 10^{-6}$ – $10 \times 10^{-6}$  M.

### 2.4. Gravimetric measurements

The gravimetric method (weight loss) is probably the most widely used method of inhibition assessment (Musa et al., 2010; Khadom et al., 2010; Bouklah et al., 2006; Mercer, 1985). The simplicity and reliability of the measurement offered by the weight loss method are such that the technique forms the baseline method of measurement in many corrosion monitoring programmes (Afidah and Kassim, 2008). Weight loss measurements were conducted under total immersion using 250 mL capacity beakers containing 200 mL test solution at 303–333 K maintained in a thermostated water bath. The mild steel coupons were weighed and suspended in the beaker with the help of rod and hook. The coupons were retrieved at 2 h interval progressively for 10 h, washed thoroughly in 20% NaOH solution containing 200 g/l of zinc dust (Obot and Obi-Egbedi, 2010b) with bristle brush, rinsed severally in deionized water, cleaned, dried in acetone, and re-weighed. The weight loss, in grams, was taken as the difference in the weight of the mild steel coupons before and after immersion in different test solutions. Then the tests were repeated at different temperatures. In order to get good reproducibility, experiments were carried out in triplicate. In this present study, the standard deviation values among parallel triplicate experiments were found to be smaller than 5%, indicating good reproducibility. A visual examination was carried out after the weight loss measurements were over. It should be noted that in the absence of inhibitor the uniform corrosion attack was observed, while on the other hand in the presence of XEN, such an attack was not observed: therefore the surface area was bright and did not present any corrosion form which is an indication that no attack has occurred on the surface area of mild steel.

The corrosion rate ( $\rho$ ) in  $g\ cm^{-2}\ h^{-1}$  was calculated from the following equation (Umoren et al., 2010):

$$\rho = \frac{\Delta W}{St} \quad (3)$$

where  $W$  is the average weight loss of three mild steel sheets,  $S$  the total area of one mild steel specimen, and  $t$  is the immersion time (10 h). With the calculated corrosion rate, the inhibition efficiency (% $I$ ) was calculated as follows (Umoren et al., 2009a,b):

$$\%I = \left( \frac{\rho_1 - \rho_2}{\rho_1} \right) \times 100 \quad (4)$$

where  $\rho_1$  and  $\rho_2$  are the corrosion rates of the mild steel coupons in the absence and presence of inhibitor, respectively.

### 2.5. Spectrophotometric measurements

UV-visible absorption spectrophotometric method was carried out on the prepared mild steel samples after immersion in 0.5 M  $H_2SO_4$  with and without addition of  $10 \times 10^{-6}$  M of xanthene at 303 K for 3 days. All the spectra measurements were carried out using a Perkin-Elmer UV-visible Lambda 2 spectrophotometer.

## 2.6. Computational details

B3LYP, a version of the DFT method that uses Becke's three parameter functional (B3) and includes a mixture of HF with DFT exchange terms associated with the gradient-corrected correlation functional of Lee, Yang and Parr (LYP) Lee et al., 1988, was used in this paper to carry out quantum calculations. Then, full geometry optimization together with the vibrational analysis of the optimized structures of the inhibitor was carried out at the (B3LYP/6-31G (d) level of theory using Spartan'06 V112 program package (Spartan and Wavefunction, 2006) in order to determine whether they correspond to a maximum or a minimum in the potential energy curve. The theoretical parameters were calculated for xanthene molecule in aqueous phase. It is well known that the phenomenon of electrochemical corrosion occurs in liquid phase. As a result, it was necessary to include the effect of a solvent (water) in the computational calculations. In the Spartan'06 V112 program, SCRF methods (self-consistent reaction field) were used to perform calculations in solution. These methods model the solvent as a continuum of uniform dielectric constant and the solute is placed in the cavity within it.

## 3. Results and discussion

### 3.1. Weight loss and corrosion rate

Corrosion inhibition performance of organic compounds as corrosion inhibitors can be evaluated using electrochemical and chemical techniques. For the chemical methods, a weight loss measurement is ideally suited for long term immersion test. Corroborative results between weight loss and other techniques have been reported (Shukla and Quraishi, 2009; Singh and Quraishi, 2010; Fouda et al., 2006; Noor and Al-Moubaraki, 2008). Moreover, de Souza and Spinelli (2009) reported that weight loss provides more reliable results than electrochemical

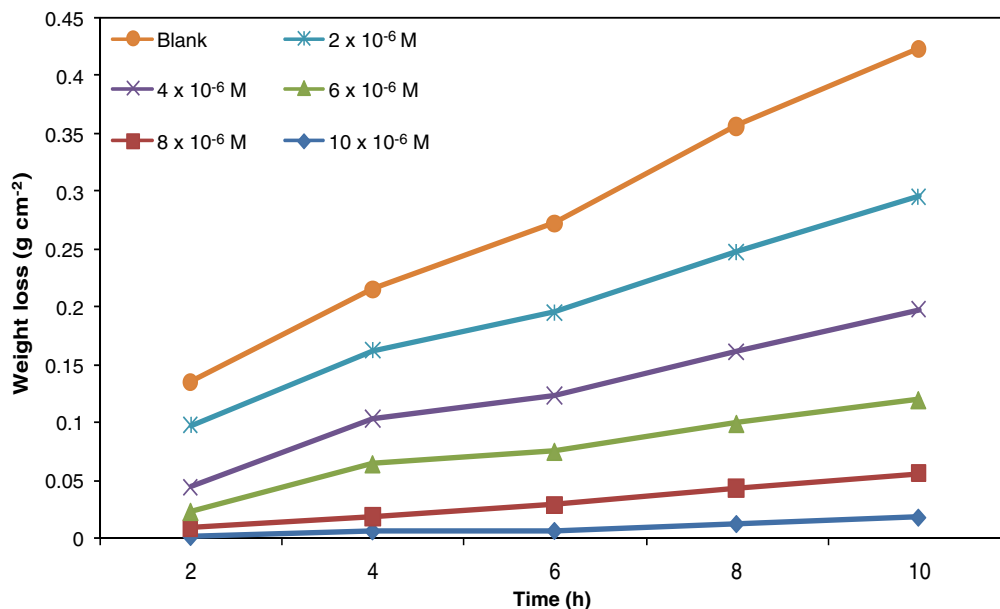
techniques for the determination of corrosion rates and inhibition efficiency.

The effect of addition of XEN at different concentrations on the corrosion of mild steel in 0.5 M H<sub>2</sub>SO<sub>4</sub> was investigated using gravimetric (weight loss) technique at temperature range of 303–333 K after 10 h of immersion period. Fig. 2 shows the plot of weight loss against time for mild steel in 0.5 M H<sub>2</sub>SO<sub>4</sub> containing XEN in 303 K. Similar plots were also obtained for other temperatures (313–333 K). The figure clearly shows that XEN actually inhibited the acid induced corrosion of mild steel as evident in the reduction in weight loss of the metal coupons in the presence of XEN compared to the free acid solution. Inspection of the figure further revealed that the loss in weight of the coupons decreases as the concentration of the inhibitor increases.

The corrosion rate values of mild steel with different concentrations of XEN in 0.5 M H<sub>2</sub>SO<sub>4</sub> at 303–333 K are shown in Table 1. The corrosion rate values decrease as the concentration of the inhibitor increases, i.e. the corrosion inhibition enhances with inhibitor concentration. This behavior is ascribed to the fact that the extent of adsorption and the coverage of inhibitor on mild steel surface increases with inhibitor concentration (Li et al., 2009a). Also, the values in Table 1 show that the corrosion rate increases with increasing temperature both in uninhibited and inhibited solutions. The corrosion rate increases more rapidly with temperature in the absence of inhibitor (Fig. 3). These results confirm that XEN acts as an efficient inhibitor in the range of temperature studied.

### 3.2. Effect of XEN concentration and temperature on inhibition efficiency

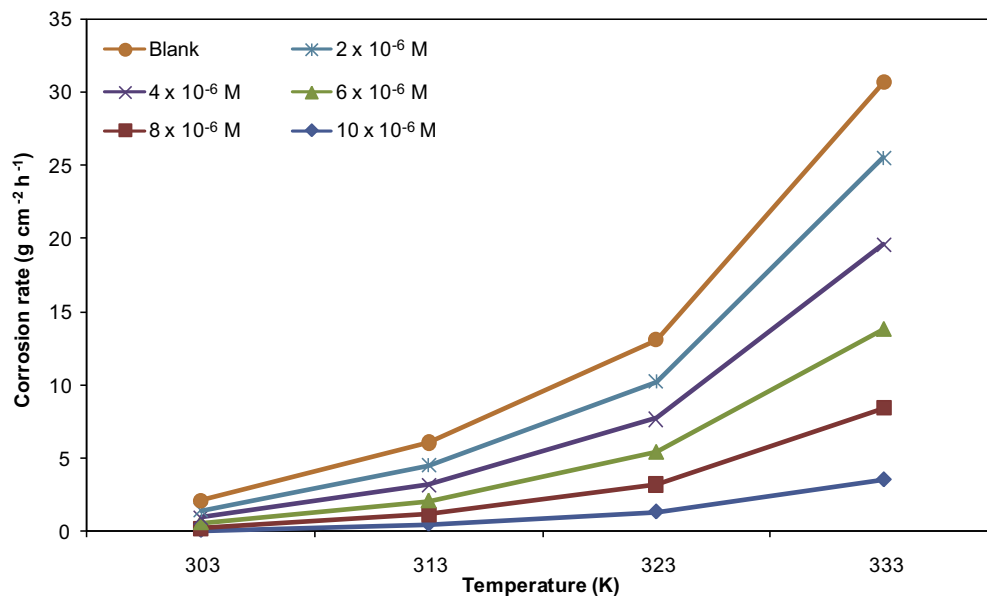
The values of inhibition efficiency obtained from the weight loss (%I) for different XEN concentrations in 0.5 M H<sub>2</sub>SO<sub>4</sub> are shown in Table 1. The (%I) increases as the concentration



**Figure 2** Variation of weight loss against time for mild steel corrosion in 0.5 M H<sub>2</sub>SO<sub>4</sub> in the presence of different concentrations of XEN at 303 K.

**Table 1** Calculated values of corrosion rate and inhibition efficiency for mild steel corrosion for mild steel in 0.5 M H<sub>2</sub>SO<sub>4</sub> in the absence and presence of XEN at 303–333 K.

| System/concentration    | Corrosion rate (mg cm <sup>-2</sup> h <sup>-1</sup> ) |       |       |       | Inhibition efficiency (%I) |       |       |       |
|-------------------------|---|-------|-------|-------|----------------------------|-------|-------|-------|
|                         | 303 K   | 313 K | 323 K | 333 K | 303 K                      | 313 K | 323 K | 333 K |
| Blank                   | 0.64  | 1.56  | 2.85  | 6.14  | –                          | –     | –     | –     |
| 2 × 10 <sup>-6</sup> M  | 0.49  | 1.38  | 2.59  | 5.96  | 23.4                       | 11.5  | 9.1   | 2.9   |
| 4 × 10 <sup>-6</sup> M  | 0.39  | 1.01  | 2.29  | 5.78  | 39.1                       | 30.1  | 19.7  | 5.8   |
| 6 × 10 <sup>-6</sup> M  | 0.32  | 0.90  | 2.19  | 5.41  | 50.0                       | 42.3  | 23.2  | 11.9  |
| 8 × 10 <sup>-6</sup> M  | 0.19  | 0.69  | 1.89  | 4.91  | 70.3                       | 55.7  | 33.7  | 20.0  |
| 10 × 10 <sup>-6</sup> M | 0.06  | 0.48  | 1.32  | 3.51  | 90.6                       | 69.2  | 53.7  | 42.8  |

**Figure 3** The relationship between corrosion rate and temperature for different concentrations of XAN.

of inhibitor increases from  $2 \times 10^{-6}$  M to  $10 \times 10^{-6}$  M. The maximum %I is about 90.63% at  $10 \times 10^{-6}$  M (303 K), which indicates that XEN is an effective inhibitor in 0.5 M H<sub>2</sub>SO<sub>4</sub>.

The influence of temperature on percentage inhibition efficiency was studied by conducting weight loss measurements at 303–333 K containing different concentrations of XEN (Table 1). Fig. 4 shows the variation of percentage inhibition efficiency with temperature. It is clear from the figure that percentage inhibition efficiency decreases with temperature. The decrease in inhibition efficiency with increase in temperature may probably be due to the increased rate of desorption of XEN from the mild steel surface at higher temperature (Li et al., 2009b).

### 3.3. Effect of temperature and activation parameters on the inhibition process

Temperature is an important parameter in studies on metal dissolution studies (de Souza and Spinelli, 2009). The corrosion rate in acid solutions, for example, increases exponentially with temperature increase because the hydrogen evolution overpotential decreases (Popova et al., 2003). To assess the effect of temperature on corrosion and corrosion inhibitive process, weight loss experiments were performed at 10 K intervals

in the temperature range 303–333 K in uninhibited acid (0.5 M H<sub>2</sub>SO<sub>4</sub>) and in inhibited solutions containing different concentrations of XEN. The results obtained for a 10 h immersion period are shown in Table 1. The relationship between the corrosion rate ( $\rho$ ) of mild steel in acidic media and temperature ( $T$ ) is often expressed by the Arrhenius equation (Noor and Al-Moubaraki, 2008):

$$\log \rho = \log A - \frac{E_a}{2.303 RT} \quad (5)$$

where  $\rho$  is the corrosion rate,  $E_a$  is the apparent activation energy,  $R$  is the molar gas constant ( $8.314 \text{ J K}^{-1} \text{ mol}^{-1}$ ),  $T$  is the absolute temperature, and  $A$  is the frequency factor. The plot of  $\log \rho$  against  $1/T$  for mild steel corrosion in 0.5 M H<sub>2</sub>SO<sub>4</sub> in the absence and presence of different concentrations of XEN is presented in Fig. 5. All calculated parameters are given in Table 2. The relationships between the temperature dependence of %I of an inhibitor and the  $E_a$  can be classified into three groups according to temperature effects (Priya et al., 2008).

- (i) %I decreases with increase in temperature,  $E_a$  (inhibited solution) >  $E_a$  (uninhibited solution).

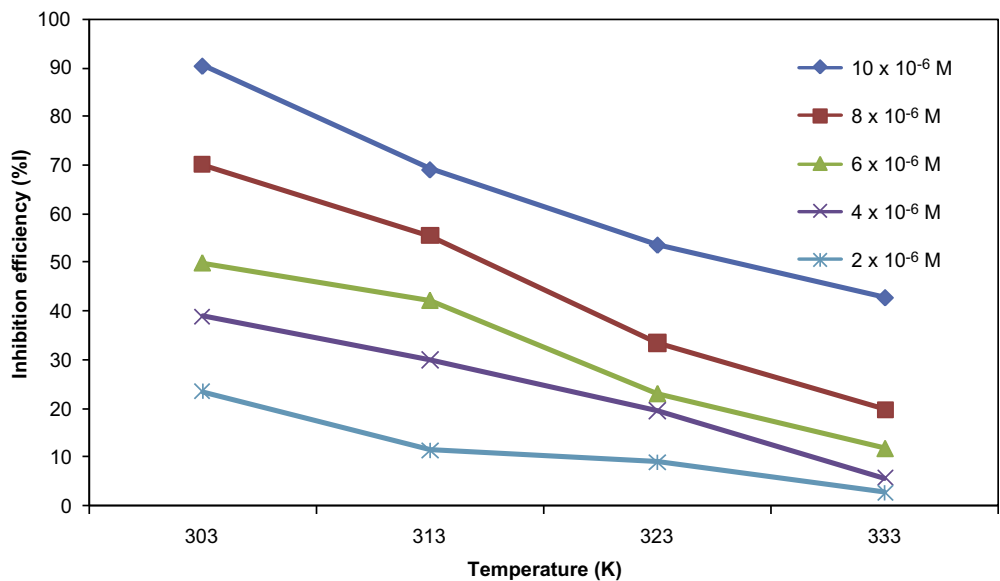


Figure 4 Variation of inhibition efficiency of XEN with temperature.

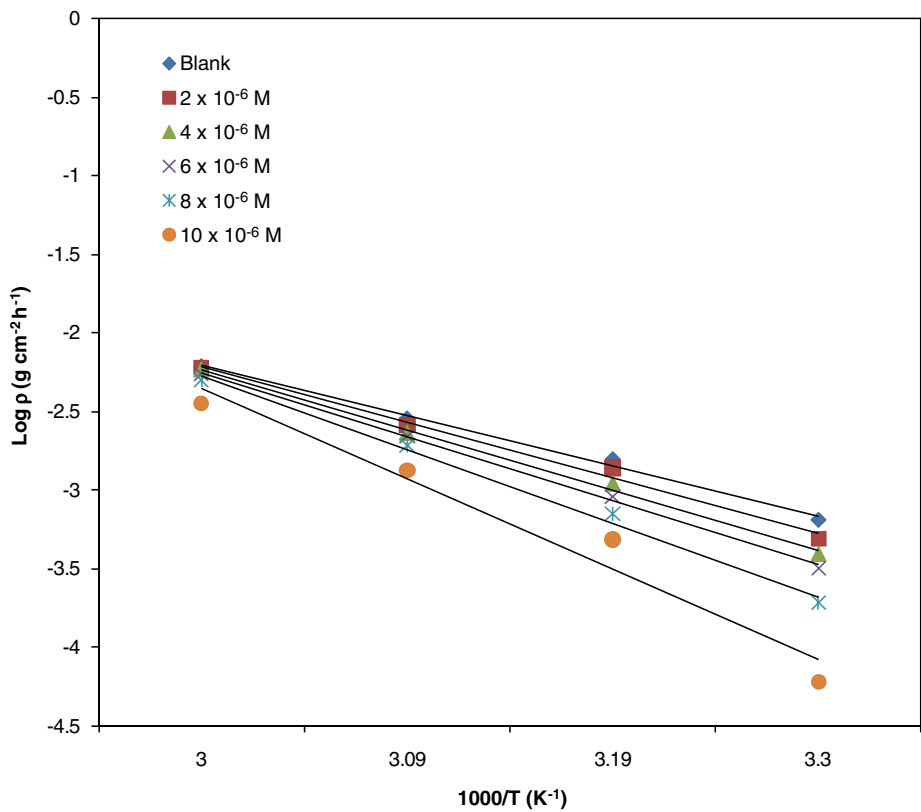


Figure 5 Arrhenius plot for mild steel corrosion in 0.5 M H<sub>2</sub>SO<sub>4</sub> in the absence and presence of different concentrations of xanthene (XEN).

- (ii) %I increases with increase in temperature,  $E_a$  (inhibited solution) <  $E_a$  (uninhibited solution).
- (iii) %I does not change with temperature,  $E_a$  (inhibited solution) =  $E_a$  (uninhibited solution).

It is clear from Table 2, that case (i) is applicable in this work, i.e.  $E_a$  in the inhibited solution is higher than that obtained for the free acid solution indicating that the corrosion reaction of mild steel is inhibited by XEN (Ebenso, 2003),

**Table 2** Activation parameters of the dissolution of mild steel in 0.5 M H<sub>2</sub>SO<sub>4</sub> in the absence and presence of different concentrations of XEN.

| C(M)                | $E_a$ (kJ mol <sup>-1</sup> ) | $\Delta H^*$ (kJ mol <sup>-1</sup> ) | $\Delta S^*$ (J mol <sup>-1</sup> K <sup>-1</sup> ) |
|---------------------|-------------------------------|--------------------------------------|---|
| Blank               | 6.12                          | 24.5                                 | -299.3  |
| $2 \times 10^{-6}$  | 6.74                          | 26.5                                 | -297.5  |
| $4 \times 10^{-6}$  | 7.33                          | 28.5                                 | -296.8  |
| $6 \times 10^{-6}$  | 7.79                          | 30.0                                 | -296.6  |
| $8 \times 10^{-6}$  | 8.94                          | 33.9                                 | -293.4  |
| $10 \times 10^{-6}$ | 10.99                         | 40.9                                 | -290.6  |

hence supports the phenomenon of physical adsorption (Umoren and Obot, 2008). Higher values of  $E_a$  in the presence of inhibitor can be correlated with increasing thickness of the double layer which enhances the  $E_a$  of the corrosion process (Singh et al., 2008). It is also an indication of a strong inhibitive action of XEN by increasing energy barrier for the corrosion process, emphasizing the electrostatic character of the inhibitor's adsorption on the mild steel surface (physisorption) Obot et al., 2010; Obot and Obi-Egbedi, 2010a; Obot and Obi-Egbedi, 2008a. According to Damaskin (1971), the value of activation energy less than 80 kJ mol<sup>-1</sup> and even smaller than 5 kJ mol<sup>-1</sup> represents physical adsorption. This assertion supports the experimental results obtained in the present work.

Experimental corrosion rate values obtained from weight loss measurements for mild steel in 0.5 M H<sub>2</sub>SO<sub>4</sub> in the absence and presence of XEN were used to gain further insight on the change of enthalpy ( $\Delta H^*$ ) and entropy ( $\Delta S^*$ ) of activation for the formation of the activation complex in the transi-

tion state using the transition state equation (Noor and Al-Moubaraki, 2008):

$$\rho = \left(\frac{RT}{Nh}\right) \exp\left(\frac{\Delta S^*}{R}\right) \exp\left(\frac{-\Delta H^*}{RT}\right) \quad (6)$$

where  $\rho$  is the corrosion rate,  $h$  is the Plank's constant ( $6.626176 \times 10^{-34}$  Js),  $N$  is the Avogadro's number ( $6.02252 \times 10^{23}$  mol<sup>-1</sup>),  $R$  is the universal gas constant and  $T$  is the absolute temperature. Fig. 6 shows the plot of  $\log \rho/T$  versus  $1/T$  for mild steel corrosion in 0.5 M H<sub>2</sub>SO<sub>4</sub> in the absence and presence of different concentrations of XEN. Straight lines were obtained with slope of  $(\Delta H^*/2.303R)$  and an intercept of  $[\log(R/Nh) + (\Delta S^*/2.303R)]$  from which the values of  $\Delta H^*$  and  $\Delta S^*$  respectively were computed and also listed in Table 2. The positive values of  $\Delta H^*$  both in the absence and presence of XEN reflect the endothermic nature of the steel dissolution process (Bentiss et al., 2007). The negative values of entropy of activation both in the absence and presence of inhibitor imply that the activated complex in the rate determining step represents an association rather than a dissociation step, meaning that a decrease in disordering takes place on going from reactants to the activated complex (Tao et al., 2009; Oguzie et al., 2008).

### 3.4. Thermodynamic consideration using statistical physics

The adsorption of an inhibitor species,  $I$ , on a metal surface,  $M$ , can be represented by a simplified equation:



Let  $M$  of the above reaction be the system in the ensemble and the solvent-containing inhibitor molecules as donor particles

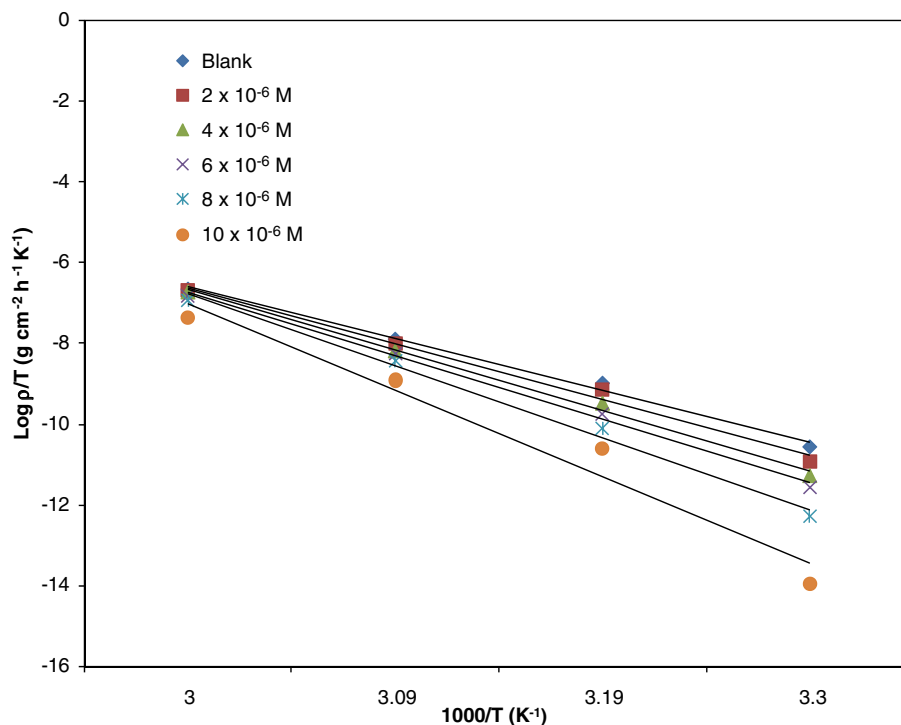


**Figure 6** Transition state plot for mild steel corrosion in 0.5 M H<sub>2</sub>SO<sub>4</sub> in the absence and presence of different concentrations of xanthene (XEN).

be the medium. The complex-forming process can be regarded as the course of distribution of donor particles to the system. So it is justifiable to extend the model of variable number of particles in statistical physics for the inhibiting process.

According to statistical Physics (Landau and Lifshitz, 1980), the probability of distribution for such kind of systems of variable number of particles is given by:

$$\varpi(i, \varepsilon) = A \exp\left(\frac{i\mu - \varepsilon_i}{\theta}\right) \quad (8)$$

where  $A$  is the normalizing coefficient,  $\mu$  the chemical potential which depends upon the temperature and concentration of the donor particles,  $i$  the number of donor particles distributed in each system,  $\theta$  the distribution modulus,  $\varepsilon_i$  the energy of the system containing  $i$  donor particles, being assumed approximately equal for the systems containing the same number  $i$  of donor particles, and  $\varepsilon_i = 0$  at  $i = 0$ .

The normalizing condition is:

$$\sum_{i=0}^n \varpi(i, \varepsilon) = 1 \quad (9)$$

or

$$A \left\{ 1 + \sum_{i=1}^n \exp\left(\frac{i\mu - \varepsilon_i}{\theta}\right) \right\} = 1 \quad (10)$$

The average number of donor particles accepted by each system is:

$$\bar{n} = \sum_{i=1}^n i \varpi(i, \varepsilon) = \sum_{i=1}^n i A \exp\left(\frac{i\mu - \varepsilon_i}{\theta}\right) \quad (11)$$

Eliminating  $A$  from Eqs. (10) and (11), we obtain:

$$\bar{n} = \frac{\sum_{i=1}^n i \exp((i\mu - \varepsilon_i)/\theta)}{1 + \sum_{i=1}^n \exp((i\mu - \varepsilon_i)/\theta)} \quad (12)$$

For inhibiting process, the  $M(I)_{\text{ads}}$  formation reaction corresponds to the distribution with  $i = 0$  or 1. The condition for which  $i = 0$  is taken to correspond to a state of complete cor-

rosion (surface coverage  $\eta = 0$  and protection efficiency  $\%I = 0$ ),  $i = 1$  to a state of complete inhibition (surface coverage  $\eta = 1$  and protection efficiency  $\%I = 100$ ). The actual occurred process of corrosion inhibition is a random distribution between  $i = 0$  and 1. So the corresponding actual protection efficiency ( $\%I$ ) are data between 0 and 100, and the actual surface coverage  $\eta$  is equal to the statistical average value for such a (0, 1) distribution, then for inhibiting process, Eq. (12) is reduced to:

$$\bar{n} = \eta = \frac{1}{1 + \exp((\varepsilon - \mu)/\theta)} \quad (13)$$

Here  $0 < \bar{n} < 1$ . Considering  $\eta$  is related to the concentration of donor particles and  $\varepsilon$  to the thermodynamic equilibrium constant of the complex-forming reaction, which is correlated to the change of free energy of adsorption  $\Delta G_{\text{ads}}^\circ$ , thus the following equation can be derived from Eq. (13) Wang et al., 2002:

$$\ln\left(\frac{1-\eta}{\eta}\right) = \frac{\Delta G_{\text{ads}}^\circ}{\theta} - \frac{RT \ln C}{\theta} \quad (14)$$

where  $C$  is the concentration of inhibitor particles.

The curve fitting of data in Table 1 to the statistical model at 303–333 K is presented in Fig. 7. Good correlation coefficient ( $R^2 > 0.95$ ) was obtained. The values of  $\theta$  and  $\Delta G_{\text{ads}}^\circ$  were calculated from the slope and intercept of Eq. (14). All the calculated parameters are given in Table 3.

The negative values of  $\Delta G_{\text{ads}}^\circ$  indicate spontaneous adsorption of XEN onto the mild steel surface (Ahmad et al., 2010)

**Table 3** Some parameters from statistical model for mild steel in 0.5 M H<sub>2</sub>SO<sub>4</sub>.

| Temperature (K) | $R^2$ | $\theta$           | $\Delta G_{\text{ads}}^\circ$ (kJ mol <sup>-1</sup> ) |
|-----------------|-------|--------------------|---|
| 303             | 0.955 | $1.27 \times 10^3$ | -31.0   |
| 313             | 0.970 | $1.54 \times 10^3$ | -30.9   |
| 323             | 0.960 | $1.93 \times 10^3$ | -30.6   |
| 333             | 0.990 | $1.47 \times 10^3$ | -30.7   |

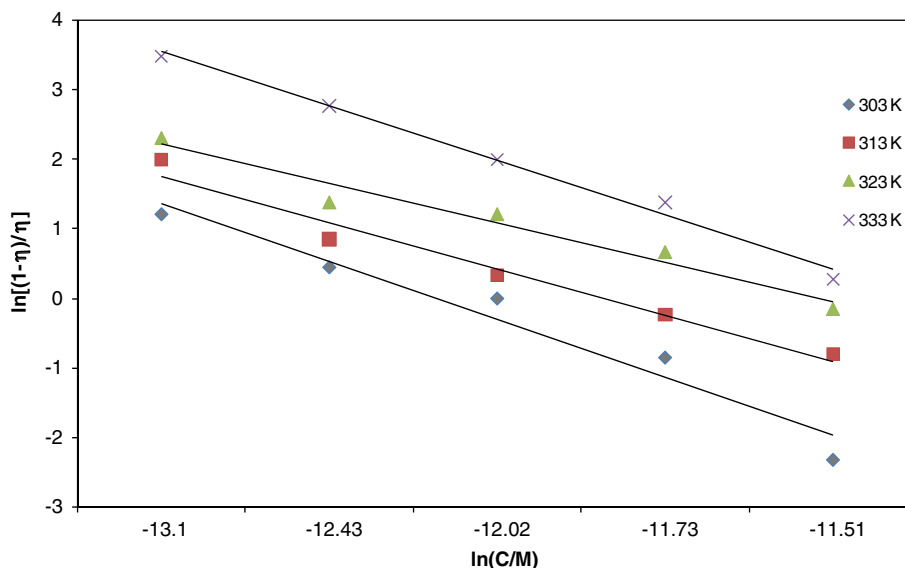


**Figure 7** Application of the statistical physics model to the corrosion protection behavior of xanthene.

and strong interactions between inhibitor molecules and the metal surface (Aljourani et al., 2010). Generally, values of  $\Delta G_{\text{ads}}^{\circ}$  up to  $-20 \text{ kJ mol}^{-1}$  are consistent with physisorption, while those around  $-40 \text{ kJ mol}^{-1}$  or higher are associated with chemisorption as a result of the sharing or transfer of electrons from organic molecules to the metal surface to form a coordinate bond (Machnikova et al., 2008). The calculated values of  $\Delta G_{\text{ads}}^{\circ}$  are greater than  $-20 \text{ kJ mol}^{-1}$  but less than  $-40 \text{ kJ mol}^{-1}$ , indicating that the adsorption mechanism of XEN on mild steel in  $0.5 \text{ M H}_2\text{SO}_4$  solution at the studied temperatures may be a combination of both physisorption and chemisorption (comprehensive adsorption) (Ahmad et al., 2010). However, physisorption was the major contributor while chemisorption only slightly contributed to the adsorption mechanism judging from the decrease of %I with increase in temperature and the higher values of  $E_a$  were obtained in the presence of inhibitor when compared to its absence.

### 3.5. Kinetics of mild steel corrosion in $\text{H}_2\text{SO}_4$ with and without xanthene

The kinetics of the mild steel corrosion in the absence and presence of different concentrations of XEN in  $0.5 \text{ M H}_2\text{SO}_4$  was studied at  $30 \text{ }^{\circ}\text{C}$  by fitting the corrosion data into different rate laws. Correlation coefficients  $R^2$  were used to determine the best rate law for the corrosion process. The rate laws considered were (Ebbing and Gammon, 2005):

$$\text{Zero-order : } W_t = kt \quad (15)$$

$$\text{First order : } \ln W_t = -kt + \ln W_o \quad (16)$$

$$\text{Second order : } 1/W_t = kt + 1/W_o \quad (17)$$

where  $W_o$  is the initial weight of mild steel,  $W_t$  is the weight loss of mild steel at time  $t$  and  $k$  is the rate constant.

By far the best result was obtained for zero-order kinetics. The plot of  $W_t$  against  $t$  which was linear (Fig. 8) with good correlation coefficients ( $R^2 > 0.846$ ) confirms a zero-order kinetics for the corrosion of mild steel in  $0.5 \text{ M H}_2\text{SO}_4$  in the absence and presence of XEN.

### 3.6. UV-visible spectroscopic study

In order to confirm the possibility of the formation of inhibitor-Fe complex, UV-visible absorption spectra obtained from  $0.5 \text{ M H}_2\text{SO}_4$  solution containing  $10 \times 10^{-6} \text{ M XEN}$  before and after 3 days of mild steel immersion are shown in Fig. 9. The electronic absorption spectra of xanthene before the immersion have absorption maxima at  $330 \text{ nm}$  due to  $\pi-\pi^*$  transition involving the whole electronic structure system of the compound with a considerable charge transfer character (Abboud et al., 2009). After 3 days of immersion, it is clearly seen that there is a blue shift (shift to a longer wavelength) and a decrease in the absorbance of this band, indicating complex formation with  $\text{Fe}^{2+}$ .

### 3.7. Quantum chemical studies

In the last few decades, theoretical investigations based on quantum chemical calculations have been proposed as a powerful tool for predicting a number of molecular parameters directly related to the corrosion inhibiting property of any chemical compound (Khaled, 2003; Bouayed et al., 1999; Jamaizadeh et al., 2008; Kutej et al., 1995). Among several theoretical methods available, the density functional theory (DFT) is one of the most important theoretical models used in explaining the science of solids and chemistry. A number of chemical concepts have been correlated within the framework of DFT (Parr and Yang, 1995). The most fundamental parameter in DFT is the electron density  $\rho(r)$  upon which all the chemical quantities are expressed (Parr and Yang, 1989). Recently, the density functional theory (DFT) has been used to analyze the characteristics of the inhibitor/surface mechanism and to describe the structural nature of the inhibitor on the corrosion process (Lashkari and Arshadi, 2004; Sein et al., 2001; Blajier and Hubin, 2004). Furthermore, DFT is considered as a very useful technique to probe the inhibitor/surface interaction as well as to analyze the experimental data. Figs. 10–13 show the optimized geometry, the HOMO density distribution, the LUMO density distribution and the Mulliken

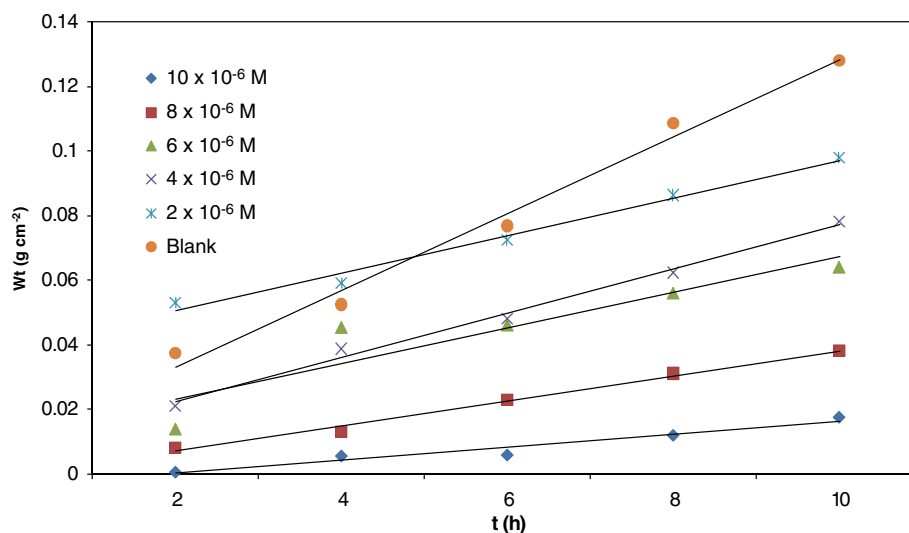


**Figure 8** The plot of  $W_t$  against  $t$  for mild steel corrosion in  $0.5 \text{ M H}_2\text{SO}_4$  with and without XEN.

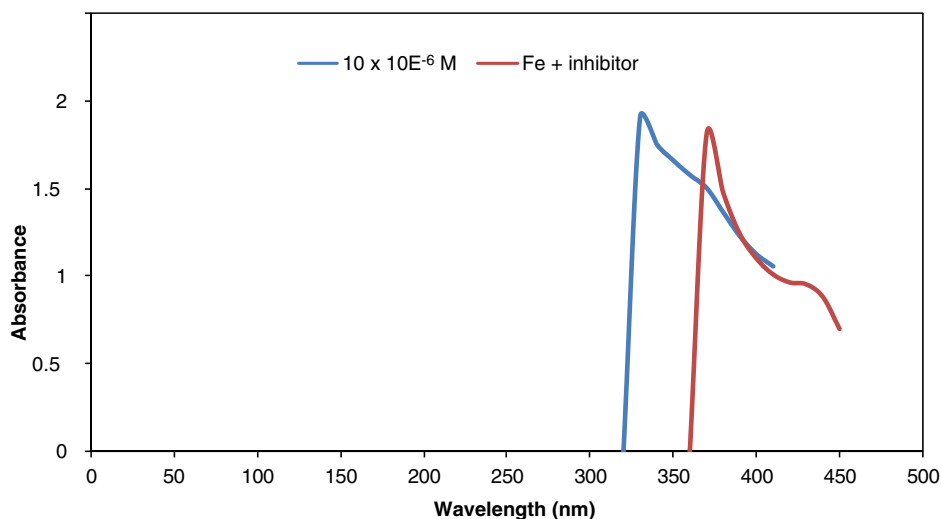


**Figure 9** UV-visible spectra of the solution containing 0.5 M  $\text{H}_2\text{SO}_4$  ( $10 \times 10^{-6}$  M) XEN before (blue) and after 3 days of mild steel immersion (red). (For interpretation of the references to colour in this figure legend, the reader is referred to the web version of this article.)

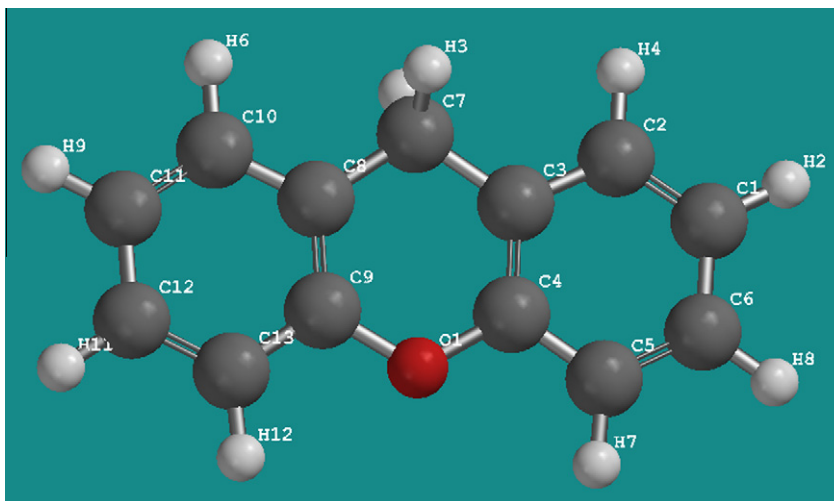


**Figure 10** Optimized structure of xanthene (XEN) (ball and stick model).

charge population analysis plots for XEN molecule in aqueous phase obtained with DFT at B3LYP/6-31G (d) level of theory.

From Figs. 11 and 12, it could be seen that XEN might have similar HOMO and LUMO distributions, which were all located on the entire xanthene moiety. This is due to the presence of oxygen atom together with several  $\pi$ -electrons on the entire molecule. This kind of structure is difficult to form chemical bond active centers, which proved the probability of physical adsorption between the interaction sites (Yan et al., 2008). Moreover, unoccupied d orbitals of Fe atom can accept electrons from the inhibitor molecule to form a coordinate bond while the inhibitor molecule can accept electrons from Fe atom with its anti-bonding orbitals to form back-donating bond.

The Mulliken charge of XEN is shown in Fig. 13. It can be seen that the most favourable sites for the interaction are C1, C2, C5, C6, C7, C10, C11, C12, C13 and O1 which has the largest negative charge. This suggests that those active centers

with excess charges could act as a nucleophilic reagent. There is a general consensus by several authors that the more negatively charged heteroatom is, the more is its ability to adsorb on the metal surface through a donor-acceptor type reaction (Obot et al., 2010; Obot and Obi-Egbedi, 2008b; Gao and Liang, 2007).

Frontier orbital theory is useful in predicting adsorption centers of the inhibitor molecules responsible for the interaction with surface metal atom (Fang and Li, 2002). Moreover, the gap between the LUMO and HOMO energy levels of the molecules was another important factor that should be considered. It has been reported that excellent corrosion inhibitors are usually those organic compounds who not only offer electrons to unoccupied orbital of the metal, but also accept free electrons from the metal (Zhao et al., 2005). It is well established in the literature that the higher the HOMO energy of the inhibitor, the greater the trend of offering electrons to unoccupied d orbital of the metal, and the higher the corrosion

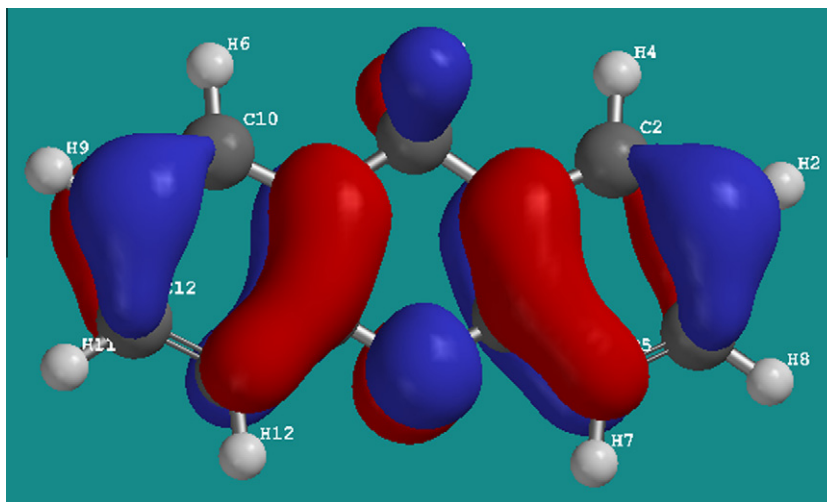


**Figure 11** The highest occupied molecular orbital (HOMO) density of xanthene (XEN) using DFT at the B3LYP/6-31G (d) basis set level.

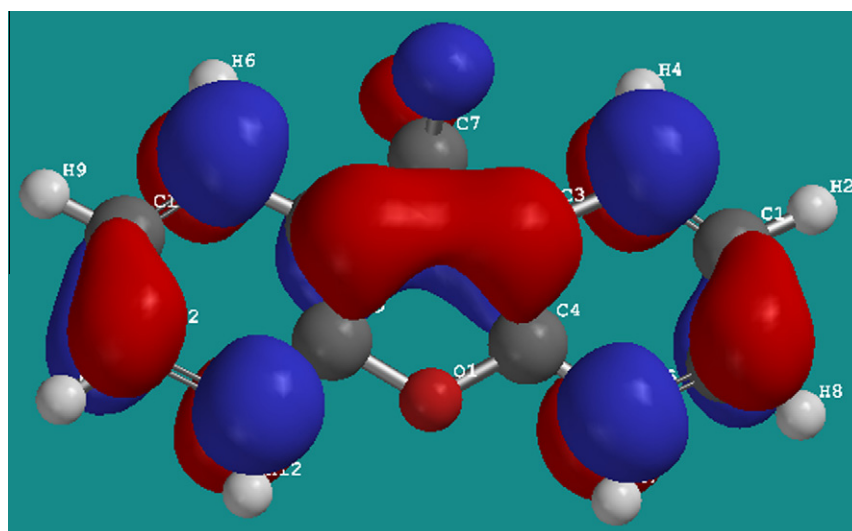


**Figure 12** The lowest unoccupied molecular orbital (LUMO) density of xanthene (XEN) using DFT at the B3LYP/6-31G (d) basis set level.

inhibition efficiency. In addition, the lower the LUMO energy, the easier the acceptance of electrons from metal surface, as the LUMO–HOMO energy gap decreased and the efficiency of inhibitor improved. Quantum chemical parameters listed in Table 4 reveal that XEN has high HOMO and low LUMO with high energy gap making it to exhibit a higher inhibitive effect obtained experimentally. Similar reports have been documented with comparable values obtained as the one reported in this work (Obot and Obi-Egbedi, 2010b; Khaled, 2008).

According to Pearson (Pearson, 1988), when two systems Fe and inhibitors are brought together electrons will flow from lower  $\chi$  (inhibitor) to higher  $\chi$ (Fe) until the chemical potentials become equal. As a first approximation, the fraction of electron transferred,  $\Delta N$ , is given by:

$$\Delta N = \frac{\chi_{\text{Fe}} - \chi_{\text{inh}}}{2(\eta_{\text{Fe}} + \eta_{\text{inh}})} \quad (18)$$

where  $\chi_{\text{Fe}}$  and  $\chi_{\text{inh}}$  denote the absolute electronegativity of Fe and the inhibitor molecule respectively;  $\eta_{\text{Fe}}$  and  $\eta_{\text{inh}}$  denote the absolute hardness of Fe and the inhibitor molecule, respectively. From Eq. (18), the Fe is the Lewis acid according to HSAB (Hard and Soft Acid and Base) theory (Pearson, 1963). The difference in electronegativity drives the electron transfer, and the sum of the hardness parameters acts as a resistance (Pearson, 1988). These quantities are related to electron affinity ( $A$ ) and ionization potential ( $I$ ) which are useful in their ability to help predict chemical behavior (Pearson, 1986).

$$\chi = \frac{I + A}{2} \quad (19)$$

$$\eta = \frac{I - A}{2} \quad (20)$$

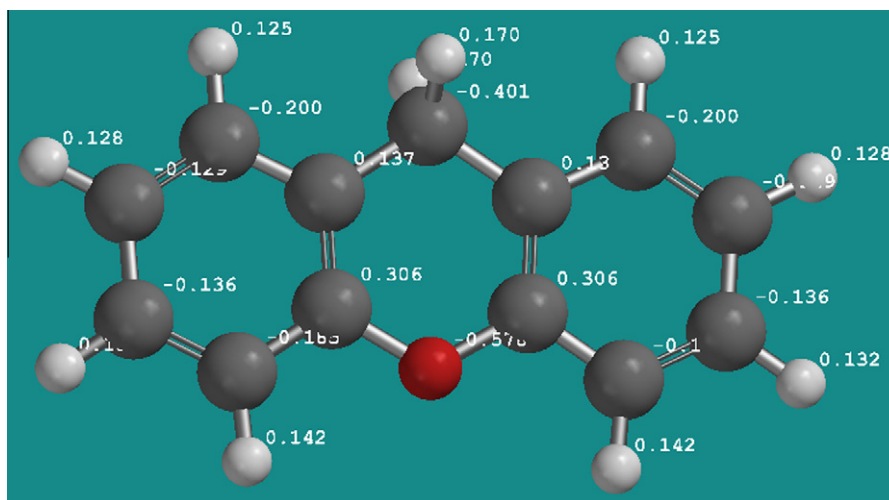


**Figure 13** Mulliken charges population analysis of xanthene (XEN) using DFT at the B3LYP/6-31G (d) basis set level.

**Table 4** Some molecular properties of xanthene calculated using DFT at the B3LYP/6-31G (d) basis set in aqueous phase.

| Molecular parameters      | Calculated values |
|---------------------------|-------------------|
| Heat of formation (au)    | -576.64           |
| Dipole moment (D)         | 1.20              |
| $E_{\text{HOMO}}$ (eV)    | -5.59             |
| $E_{\text{LUMO}}$ (eV)    | -0.32             |
| $\Delta E$ (eV)           | 5.27              |
| Volume ( $\text{\AA}^3$ ) | 197.61            |
| Area ( $\text{\AA}^2$ )   | 206.85            |
| Point group               | C2v               |
| $\Delta N$                | 0.76              |

$I$  and  $A$  are related in turn to  $E_{\text{HOMO}}$  and  $E_{\text{LUMO}}$  as follows:

$$I = -E_{\text{HOMO}} \quad (21)$$

$$A = -E_{\text{LUMO}} \quad (22)$$

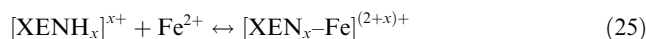
Values of  $\chi$  and  $\eta$  were calculated by using the values of  $I$  and  $A$  obtained from quantum chemical calculations. Using a theoretical  $\chi$  value of 7 eV/mol according to Pearson's electro-negativity scale (Pearson, 1988) and a global hardness  $\eta$  value of 0 eV/mol for Fe by assuming that for a metallic bulk  $I = A$  (Dewar and Thiel, 1963),  $\Delta N$ , which is the fraction of electrons transferred from inhibitor to the mild steel surface was calculated (Table 4). The value of  $\Delta N$  showed inhibition effect resulted from electrons donation. According to Lukovits et al. (2001), if  $\Delta N < 3.6$ , the inhibition efficiency increased with increasing electron donating ability at the metal surface. In this study, XEN was the donor of electrons, and the mild steel surface was the acceptor. This result supports the assertion that the adsorption of XEN on the metal surface can occur on the bases of donor-acceptor interactions between the  $\pi$  electrons of the heterocyclic compound and the vacant d-orbitals of the metal surface (Hackerman et al., 1966). The adsorption of XEN molecule on steel may be in a manner in which the plane of the inhibitor is parallel to the metal surface (Ramji et al., 2008).

### 3.8. Explanation of inhibition mechanism

From the experimental and theoretical results obtained, the inhibition effect of XEN in  $\text{H}_2\text{SO}_4$  solution can be explained as follows:



In aqueous acidic solutions, the XEN exists either as neutral molecules or in the form of cations (protonated XEN). Generally, two modes of adsorption could be considered. The neutral XEN may be adsorbed on the metal surface via the chemisorption mechanism involving the displacement of water molecules from the metal surface and the sharing of electrons between oxygen atom and iron. The XEN molecules can be adsorbed also on the metal surface on the basis of donor-acceptor interactions between  $\pi$ -electrons of the heterocycle and vacant d-orbitals of iron. On the other hand,  $\text{SO}_4^{2-}$  could adsorb on the metal surface (Bentiss et al., 2000), then the protonated XEN may adsorb through electrostatic interactions between the positive molecules and already adsorbed sulphate ions. Thus, the metal complexes of  $\text{Fe}^{2+}$  and XEN or protonated XEN might be formed as follows:



These complexes might adsorb onto steel surface by van der Waals force to form a protective film to keep the mild steel surface from corrosion. Similar mechanism has been documented (Li et al., 2009a,b).

## 4. Conclusions

The following conclusions may be drawn from the study:

- (1) Xanthene (XEN) acts as a good inhibitor for the corrosion of mild steel in 0.5 M  $\text{H}_2\text{SO}_4$ . Inhibition efficiency values increase with the inhibitor concentration but decrease with temperature. The trend of inhibition

efficiency with temperature and the increase in the activation energy in the presence of XEN suggest physical adsorption mechanism.

- (2) The Gibbs free energy for the adsorption process calculated using statistical physics is negative indicating that the process is spontaneous.
- (3) A zero-order kinetics relationship with respect to the mild steel was obtained with and without XEN from the kinetic treatment of the data.
- (4) UV-visible spectrophotometric studies clearly reveal the formation of Fe–XEN complex which may be responsible for the observed inhibition.
- (5) Data obtained from quantum chemical calculations using DFT at the B3LYP/6-31G (d) level of theory were correlated to the inhibitive effect of xanthene.

## References

- Abboud, Y., Abourriche, A., Saffaj, T., Berrada, M., Charrouf, M., Bennamara, A., Hannache, H., 2009. *Desalination* 237, 175.
- Afidah, A.R., Kassim, J., 2008. *Recent Patents Mater. Sci.* 1, 223.
- Ahamad, I., Quraishi, M.A., 2010. *Corros. Sci.* 52, 651.
- Ahamad, I., Prasad, R., Quraishi, M.A., 2010. *Corros. Sci.* 52, 933.
- Ahamad, I., Prasad, R., Quraishi, M.A., 2010. *Corros. Sci.* 52, 1472.
- J. Aljourani, M.A. Golozar, K. Raeissi, *Mater. Chem. Phys.* (2010), doi:10.1016/j.matchemphys.2010.01.040.
- Ashassi-Sorkhabi, H., Masoumi, B., Ejbari, P., Asghari, E., 2009. *J. Appl. Electrochem.* 39, 1497.
- Benabdellah, M., Hammouti, B., 2005. *Appl. Surf. Sci.* 252, 1657.
- Bentiss, F., Traisnel, M., Lagrenee, M., 2000. *Appl. Surf. Sci.* 161, 196.
- Bentiss, F., Traisnel, M., Lagrenee, M., 2000. *Corros. Sci.* 42, 127.
- Bentiss, F., Bouanis, M., Mernari, B., Traisnel, M., Vezin, H., Lagrenee, M., 2007. *Appl. Surf. Sci.* 253, 3696.
- Blajier, O., Hubin, A., 2004. *Electrochim. Acta* 49, 2761.
- Bouayed, M., Rabaa, H., Srhiri, A., Saillard, J.Y., Bachir, A.B., Le Beuze, A., 1999. *Corros. Sci.* 41, 501.
- Bouklah, M., Hammouti, B., Lagrenee, M., Bentiss, F., 2006. *Corros. Sci.* 48, 2831.
- Damaskin, B.B., 1971. *Adsorption of Organic Compounds on Electrodes*. Plenum Press, New York, p. 221.
- de Souza, F.S., Spinelli, A., 2009. *Corros. Sci.* 51, 642.
- Dewar, M.J.S., Thiel, W., 1963. *J. Am. Chem. Soc.* 85, 3533.
- Ebbing, D.D., Gammon, S.D., 2005. *General Chemistry*. Houghton Mifflin Company, Boston.
- Ebenso, E.E., 2003. *Mater. Chem. Phys.* 79, 58.
- Ebenso, E.E., Alemu, H., Umoren, S.A., Obot, I.B., 2008. *Int. J. Electrochem. Sci.* 4, 1325.
- El-Naggar, M.M., 2007. *Corros. Sci.* 49, 2236.
- Fang, J., Li, J., 2002. *J. Mol. Struct. Theochem.* 593, 197.
- Fontana, M.G., 1986. *Corrosion Engineering*, third ed. McGraw-Hill, Singapore.
- Fouda, A.S., Al-Sarawy, A.A., El-Katori, E.E., 2006. *Desalination* 201, 1.
- Gao, G., Liang, C., 2007. *Electrochim. Acta* 52, 4554.
- Hackerman, N., Snively Jr., E., Payne Jr., J.S., 1966. *J. Appl. Electrochem.* 113, 677.
- Jamaizadeh, E., Jafari, A.H., Hosseini, S.M.A., 2008. *J. Mol. Struct. Theochem.* 870, 23.
- Jones, D.A., 1992. *Principles and Prevention of Corrosion*. Macmillan, New York.
- Khadom, A.A., Yaro, A.S., Kadum, A.H., 2010. *J. Taiwan Ins. Chem. Eng.* 41, 122.
- Khaled, K.F., 2003. *Electrochim. Acta* 48, 2493.
- Khaled, K.F., 2008. *Appl. Surf. Sci.* 54, 4345.
- Kutej, P., Vosta, J., Pancir, J., Hackerman, N., 1995. *J. Electrochem. Soc.* 142, 1847.
- Landau, L.D., Lifshitz, E.M., 1980. *Statistical Physics*. Pergamon Press, Oxford, p. 107.
- Lashkari, M., Arshadi, M.R., 2004. *J. Chem. Phys.* 299, 131.
- Lebrini, M., Bentiss, F., Vezin, H., Lagrenee, M., 2006. *Corros. Sci.* 48, 1291.
- Lee, C., Yang, W., Parr, R.G., 1988. *Phys. Rev.* B37, 785.
- Li, X., Deng, S., Fu, H., Li, T., 2009a. *Electrochim. Acta* 54, 4089.
- Li, X., Deng, S., Fu, H., Mu, G., 2009b. *Corros. Sci.* 51, 620.
- Lukovits, I., Lalman, E., Zucchi, F., 2001. *Corrosion* 57, 3.
- Machnikova, E., Whitmire, K.H., Hackerman, N., 2008. *Electrochim. Acta* 53, 6024.
- Mercer, A.D., 1985. *Br. Corros. J.* 20 (2), 61.
- Musa, A.Y., Khadom, A.A., Kadum, A.H., Mohamad, A.B., Takriff, M.S., 2010. *J. Taiwan Ins. Chem. Eng.* 41, 126.
- Noor, E.A., Al-Moubaraki, A.H., 2008. *Mater. Chem. Phys.* 110, 145.
- Obot, I.B., 2009. *Portugaliae Electrochim. Acta* 27 (5), 539.
- Obot, I.B., Obi-Egbedi, N.O., 2008a. *Surf. Rev. Lett.* 15 (6), 903.
- Obot, I.B., Obi-Egbedi, N.O., 2008b. *Colloid. Surf. A: Physicochem. Eng. Aspects* 330, 207.
- Obot, I.B., Obi-Egbedi, N.O., 2009. *Corros. Sci.* 52, 276.
- Obot, I.B., Obi-Egbedi, N.O., 2010a. *Corros. Sci.* 52, 282.
- Obot, I.B., Obi-Egbedi, N.O., 2010b. *Corros. Sci.* 52, 198.
- Obot, I.B., Obi-Egbedi, N.O., 2010c. *Corros. Sci.* 52, 657.
- Obot, I.B., Obi-Egbedi, N.O., Umoren, S.A., 2009. *Int. J. Electrochem. Sci.* 4, 863.
- Obot, I.B., Obi-Egbedi, N.O., Odozi, N.W., 2010. *Corros. Sci.* 52, 923.
- Oguzie, E.E., Njoku, V.O., Enenebeaku, C.K., Akalezi, C.O., Obi, C., 2008. *Corros. Sci.* 50, 3480.
- Parr, R.G., Yang, W., 1989. *Density Functional Theory of Atoms and Molecules*. Oxford University Press, Oxford.
- Parr, R.G., Yang, W., 1995. *Rev. Phys. Chem.* 46, 701.
- Pearson, R.G., 1963. *J. Am. Chem. Soc.* 85, 3533.
- Pearson, R.G., 1986. *Proc. Natl. Acad. Sci.* 83, 8440.
- Pearson, R.G., 1988. *Inorg. Chem.* 27, 734.
- Popova, A., Sokolova, E., Christov, M., 2003. *Corros. Sci.* 45, 33.
- Priya, A.R.S., Muralidharam, V.S., Subramania, A., 2008. *Corrosion* 64, 541.
- Ramji, K., Cairns, D.R., Rajeswari, S., 2008. *Appl. Surf. Sci.* 252, 4483.
- Sein, L.T., Wei, Y., Jansen, S.A., 2001. *Comput. Theor. Polym. Sci.* 11, 83.
- Shukla, S.K., Quraishi, M.A., 2009. *Corros. Sci.* 51, 1007.
- Singh, A.K., Quraishi, M.A., 2010. *Corros. Sci.* 52, 152.
- Singh, M.R., Bhrra, K., Singh, G., 2008. *Port. Electrochim. Acta* 26 (6), 479.
- Solomon, M.M., Umoren, S.A., Udoso, I.I., Udoh, A.P., 2010. *Corros. Sci.* 52 (4), 1317.
- (Spartan,06 Wavefunction, Inc. Irvine), CA: Y. Shao, L.F. Molnar, Y. Jung, J. Kussmann, C. Ochsenfeld, S.T. Brown, A.T.B. Gilbert, L.V. Slipchenko, S.V. Levehenko, D.P. O'Neill, R.A. DiStasio Jr., R.C. Lochan, T.Wang, G.J.O. Beran, N.A. Besley, J.M. Herbert, C.Y. Lin, T. Van Voorhis, S.H. Chien, A. Sodt, R.P. Steele, V.A. Rassolov, P.E. Maslen, P.P. Korambath, R.D. Adamson, B. Austin, J. Baker, E.F.C. Byrd, H. Dachsel, R.J. Doerksen, A. Dreuw, B.D. Dunietz, A.D. Dutoi, T.R. Furlani, S.R. Gwaltney, A. Heyden, S. Hirata, C.P. Hsu, G. Kedziora, R.Z. Khaliullin, P.Klunzinger, A.M. Lee, M.S. Lee, W.Z. Liang, I. Lotan, N. Nair, B. Peters, E.I. Proynov, P.A. Pieniazek, Y.M. Rhee, J. Ritchie, E. Rosta, C.D. Sherrill, A.C. Simmonett, J.E. Subotnik, H.L. Woodcock III, W. Zhang, A.T. Bell, A.K. Chakraborty, D.M. Chipman, F.J. Keil, A. Warshel, W.J. Hehre, H.F. Schaefer, J. Kong, A.I. Krylov, P.M.W. Gill, M. Head-Gordon, *Phys. Chem. Chem. Phys.* 8 (2006) 3172.
- Tao, Z., Zhang, S., Li, W., Hou, B., 2009. *Corros. Sci.* 51, 2588.
- Umoren, S.A., Ebenso, E.E., 2007. *Mater. Chem. Phys.* 106, 393.
- Umoren, S.A., Obot, I.B., 2008. *Surf. Rev. Lett.* 15 (3), 277.

- Umoren, S.A., Obot, I.B., Ebenso, E.E., Obi-Egbedi, N.O., 2009a. *Desalination* 247, 561.
- Umoren, S.A., Obot, I.B., Obi-Egbedi, N.O., 2009b. *J. Mater. Sci.* 44, 274.
- Umoren, S.A., Solomon, M.M., Udousoro, I.I., Udoh, A.P., 2010. *Cellulose* 17, 635.
- Wang, H.L., Fan, H.B., Zheng, J.S., 2002. *Mater. Chem. Phys.* 77, 655.
- Wikipedia encyclopedia, <http://en.wikipedia.org/wiki/xanthene>, 2010.
- Yan, Y., Li, W., Cai, L., Hou, B., 2008. *Electrochim. Acta* 53, 5953.
- Zhao, P., Liang, Q., Li, Y., 2005. *Appl. Surf. Sci.* 252, 1596.